Formation and evolution of far-field diffraction patterns of divergent and convergent Gaussian beams passing through self-focusing and self-defocusing media

INSTITUTE OF PHYSICS PUBLISHING JOURNAL OF OPTICS A: PURE AND APPLIED OPTICS
J. Opt. A: Pure Appl. Opt. **7** (2005) 409–415 doi:10.1088/1464-4258/7/8/011

Formation and evolution of far-field diffraction patterns of divergent and convergent Gaussian beams passing through self-focusing and self-defocusing media

Luogen Deng[1], **Kunna He, Tiezhong Zhou and Chengde Li**

Department of Physics, Beijing Institute of Technology, Beijing 100081, People's Republic of China

E-mail: luogen@bit.edu.cn

Received 2 March 2005, accepted for publication 18 May 2005
Published 15 July 2005
Online at stacks.iop.org/JOptA/7/409

Abstract
The formation and the evolution of the far-field patterns of the Gaussian beams passing through a thin self-focusing medium and a thin self-defocusing medium are studied using the Fresnel–Kirchhoff diffraction theory, and the effects of the different Kerr media and the different Gaussian beams on the far-field pattern formation and evolution are analysed by taking into consideration both the change in the additional phase shift induced by the refractive index and the change in the sign of the radius of wavefront curvature of the laser beam passing through the nonlinear medium. Our results show that, when either the divergent Gaussian beam passes through the self-defocusing medium or the convergent Gaussian beam passes through the self-focusing medium, the far-field intensity distribution pattern is a series of thick diffraction rings with a central dark spot; while, when either the divergent Gaussian beam traverses the self-focusing medium or the convergent Gaussian beam traverses the self-defocusing medium, the far-field intensity distribution pattern is a series of thin diffraction rings with a central bright spot. Our results also show that whether the central dark spot or the central bright spot occurs depends mainly on the sign of the product of the additional phase shift and the radius of the wavefront curvature. When the sign is negative, that is, when the divergent Gaussian beam passes through the self-defocusing media, or the convergent Gaussian beam passes through the self-focusing media, the central dark spot surrounded by the thick diffraction rings will emerge in the far field; while, when the sign is positive, that is, when the divergent Gaussian beam traverses the self-focusing media, or the convergent Gaussian beam passes through the self-defocusing media, the central bright spot with the thin diffraction rings will occur in the far field. The difference between the diffraction patterns is attributed to the interplay of the strong spatial self-phase modulation caused by the refractive index change of the medium and the changes in sign of the radius of the wavefront curvature of the incident Gaussian beam. The results obtained in this paper are of significance to the design of practical nonlinear optical limiters for the eye or sensor protection and many other applications.

Keywords: nonlinear optics, Gaussian beam, spatial self-phase modulation, diffraction pattern, self-focusing/defocusing, nonlinear medium, additional phase shift, wavefront curvature

(Some figures in this article are in colour only in the electronic version)

[1] Author to whom any correspondence should be addressed.

1. Introduction

When the Gaussian beam passes through a nonlinear medium, a concentric ring intensity distribution pattern tends to form in the far field. This phenomenon has aroused wide interest among researchers since Callen *et al* [1] observed first the far-field annular intensity distribution of a He–Ne laser beam passing through the nonlinear liquid CS_2 in 1967. A similar phenomenon in the liquid crystals was observed by Durbin *et al* [2] in 1981. Afterwards, the far-field annular diffraction patterns were found in many nonlinear media, one after another. The phenomena observed in experiments are mostly sets of concentric rings [1–4]. The main difference between these patterns is that the central area of some patterns is dark, while the central zone of the other patterns is bright. In addition, some terms such as the 'thick diffraction ring' and the 'thin diffraction ring' were used by various authors [5]. Recently, the so-called doughnut laser beam with the central dark spot and a single outer bright ring has also attracted special interest because of its possible applications in fields such as optical limiting [6, 7], laser writing and drilling, measurement of thermal diffusivity, trapping and guiding of atoms [8, 9], laser manipulation of microscopic dielectric and metal objects [10, 11]. For years, researchers tried hard to explain these phenomena on the basis of the experimental observations. In 1984, Santamato *et al* [4] gave a good explanation for the far-field diffraction pattern with a central bright spot observed behind a liquid crystal film. They described the spatial self-phase modulation produced by the laser passing through the liquid crystal film by means of a diffractive integral, and discussed the effect of the wavefront curvature on the ring structure. Later on, Yu *et al* [12] analysed the far-field dark spot phenomenon of the divergent Gaussian beam passing through the absorptive self-defocusing media by means of the coupled field–matter equations and regarded it as the result of the co-action of the beam wavefront curvature and the spatial self-phase modulation caused by the thermally induced refractive index change, but they did not discuss the far-field intensity distribution of the divergent Gaussian beam traversing the absorptive self-focusing media.

Although the interpretation and the analysis given by the above authors seem essentially correct, several questions remained without clear answers: Why can one observe two different kinds of far-field diffraction patterns in the experiments? What are the conditions under which the central dark spot and the central bright spot form? What are the thick diffraction rings and the thin diffraction rings? What are the relations between the thick or thin diffraction ring pattern and the diffraction ring patterns with the central dark or bright spots? In order to clarify these questions, we studied the far-field diffraction pattern formation and evolution of the Gaussian beam passing through the optically thin nonlinear media by numerical simulation using the Fresnel–Kirchhoff diffraction formula and analysed the conditions under which the different diffraction patterns occur. The simulation results show that, when a divergent Gaussian beam is transmitted through a self-defocusing nonlinear medium or a convergent Gaussian beam passes through a self-focusing nonlinear medium, the intensity distribution pattern in the far field is a series of thick diffraction rings with a central dark spot and a larger distribution size; while when a divergent Gaussian beam passes through a self-focusing nonlinear medium or a convergent Gaussian beam traverses a self-defocusing nonlinear medium the intensity distribution pattern in the far field is a series of thin diffraction rings with a central bright spot and a narrower distribution size. Under the condition that the laser input is given, the emergence of the diffraction ring pattern with the central dark spot effectively limits the light energy entering the detector. Therefore, the phenomenon of the far-field dark spot of the transmission of the Gaussian beam through the nonlinear medium can be employed to perform optical limiting [13, 14].

2. Theory

In nonlinear optical phenomena the spatial self-phase modulation on the cross-section of the Gaussian beam emerges as a kind of wavefront distortion. For a thin nonlinear medium, although the change in the radial size of the Gaussian beam caused by the self-focusing and defocusing is negligible, the spatial self-phase modulation induced by the self-action is rather appreciable. For a beam with a Gaussian profile the phase increment $\Delta\phi(r)$ has a bell-shaped distribution of which the centre is at $r = 0$. If $[\Delta\phi(r)]_{\max}$ is much larger than 2π, a set of concentric rings will appear on the far-field observation screen as the Gaussian beam is transmitted through the nonlinear medium. To quantitatively study the law of the far-field diffraction pattern formation, we start first with the derivation process for the relevant theoretical formula in the following.

Consider a beam with a TEM_{00} Gaussian intensity profile propagating through a nonlinear medium of thickness L along the direction of the Z-axis, and the beam-waist position taken as the origin of the coordinate system. The complex amplitude of the light electric field on the entrance plane of the medium can be written as

$$E(r, z_0) = E(0, z_0) \exp\left(-\frac{r^2}{w_p^2}\right) \exp\left(-\frac{ik_0 n_0 r^2}{2R}\right) \qquad (1)$$

where r is the radial coordinate, z_0 is the position coordinate of the medium entrance plane, k_0 is the free-space wavenumber, n_0 is the refractive index of the air around the medium, w_p is the beam radius at the medium entrance plane, R is the radius of wavefront curvature in the corresponding position. $E(0, z_0)$, which is the electric field of the entrance-plane centre of the medium, is constant once the position of the medium is fixed. Because of the light absorption of the nonlinear medium and the third-order nonlinear optics effects, an additional refractive index distribution being proportional to the light intensity, $\Delta n(z, r)$, occurs in the light action area in the medium. Therefore, when the Gaussian beam with the wavelength λ denoted by equation (1) is propagated through the nonlinear medium, the transverse additional phase shift induced on the exit plane of the medium can be expressed as

$$\Delta\phi(r) = k_0 \int_{z_0}^{z_0+L} \Delta n(z, r)\, dz. \qquad (2)$$

Suppose that the medium is optically thin and its nonlinear absorption is negligible; the complex amplitude of the electric

field on the exit plane of the medium can be expressed as

$$E(r, z_0 + L) = E(0, z_0) \exp\left(-\frac{\alpha L}{2}\right) \exp\left(-\frac{r^2}{w_p^2}\right) \exp(-i\phi(r)) \tag{3}$$

where α is the linear absorption coefficient of the nonlinear medium and

$$\phi(r) = k_0 \frac{n_0 r^2}{2R} + \Delta\phi(r) = k_0 \left[\frac{n_0 r^2}{2R} + \int_{z_0}^{z_0+L} \Delta n(z, r)\, dz\right]$$
$$\approx k_0 \frac{n_0 r^2}{2R} + \Delta\phi_0(z_0) \exp\left(-\frac{2r^2}{w_p^2}\right) \tag{4}$$

is, on the exit plane of the medium, the total phase shift which is comprised of the Gaussian phase shift determined by the curvature radius R and the transverse additional phase shift produced by the propagation of the beam through the medium. In equation (4), $\Delta\phi_0(z_0)$ is the peak nonlinear phase shift induced in the Gaussian beam when the entrance surface of the medium is positioned at z_0. It is the co-action of the Gaussian phase shift and the transverse additional phase shift that determines the far-field intensity distribution of the Gaussian beam passing through the nonlinear medium.

When the optical field on the exit plane of the medium is freely propagated through the space, the corresponding far-field intensity distribution can be expressed, by means of the Fraunhofer approximation of the Fresnel–Kirchhoff diffraction formula [15], as

$$I = \left|\frac{1}{i\lambda D}\right|^2 \left|\int_0^{\infty} \int_0^{2\pi} E(0, z_0) \exp\left(-\frac{\alpha L}{2}\right)\right.$$
$$\left. \times \exp(-ik_0 r\theta \cos\varphi) \exp\left[-\frac{r^2}{w_p^2} - i\phi(r)\right] r\, dr\, d\varphi\right|^2 \tag{5}$$

where θ is the far-field diffraction angle, φ is the angular coordinate on the exit plane of the medium under the polar coordinate system, D is the distance from the exit plane of the medium to the far-field observational plane. The radial coordinate ρ in the far-field observational plane is related to the far-field diffraction angle θ by

$$\rho = D\theta. \tag{6}$$

Using the property of the first-kind zero-order Bessel function as an even function, that is

$$J_0(x) = \frac{1}{2\pi} \int_0^{2\pi} \exp(ix\cos\varphi)\, d\varphi$$
$$= \frac{1}{2\pi} \int_0^{2\pi} \exp(-ix\cos\varphi)\, d\varphi, \tag{7}$$

equation (5) can be rewritten as

$$I = I_0 \left|\int_0^{\infty} J_0(k_0\theta r) \exp\left[-\frac{r^2}{w_p^2} - i\phi(r)\right] r\, dr\right|^2 \tag{8}$$

where $I_0 = 4\pi^2 |E(0, z_0) \exp(-\alpha L/2)/i\lambda D|^2$. Equation (8) will be exploited to examine the law of the far-field diffraction pattern formation in the following section.

When a laser beam acts on a nonlinear medium, the reasons for which the refractive index change are various and the mechanisms behind the changes in the refractive index are not completely the same. For the photorefractive effect, the change in the refractive index of the nonlinear media has nothing to do with the light intensity, and the light intensity affects merely the speed of the photorefractive process, while for the optical Kerr effect, the change in the refractive index is proportional to the light intensity. In this paper, equation (8) actually reflects the effect of the additional phase shift caused by the refractive index change on the far-field diffraction pattern, and is suitable for nonlinear media whose refractive index change is proportional to the light intensity ($\Delta n = n_2 I$, where n_2 is the coefficient of the nonlinear refractive index of the medium). As a matter of fact, besides the optical Kerr effect, there are several physical mechanisms [16–19] which can induce a refractive index change proportional to the light intensity in the media. According to equation (8), no matter what kind of mechanism works, the far-field diffraction patterns will be alike as long as the additional phase shifts are identical. In other words, the effect of the additional phase shift caused by the refractive index change on the far-field diffraction pattern is only relevant to the magnitude of the additional phase shift produced after the beam passes through the medium and is not relevant to the mechanism by which the change in the refractive index occurs. Anyway, equation (8) can be used to calculate the far-field intensity distribution led to by the refractive index change being proportional to the light intensity induced by various different mechanisms.

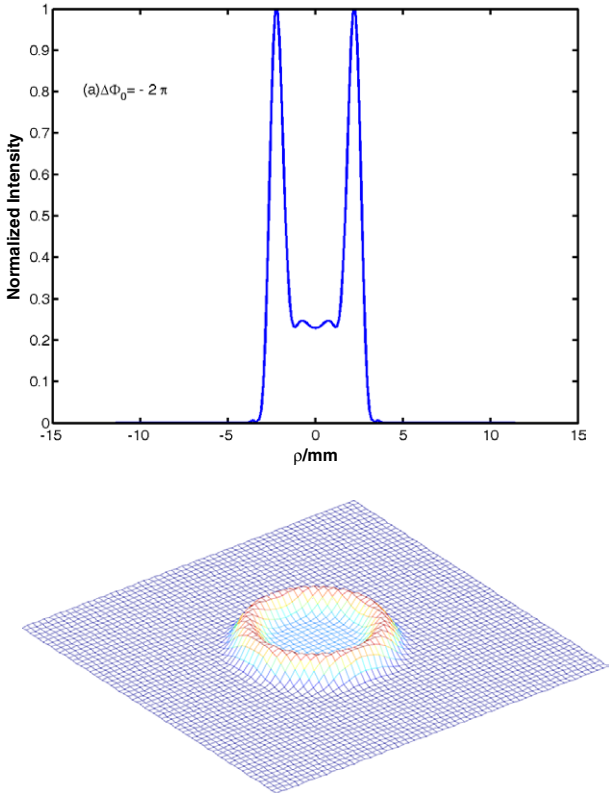

Figure 1. Calculation of the intensity distribution in the far field when the peak-value phase shift $\Delta\phi_0(z_0) = -2\pi$ and the curvature radius $R = 1.33$ m.

3. Simulation method and results

Generally, the change in the refractive index Δn in the nonlinear medium will usually take place when the Gaussian

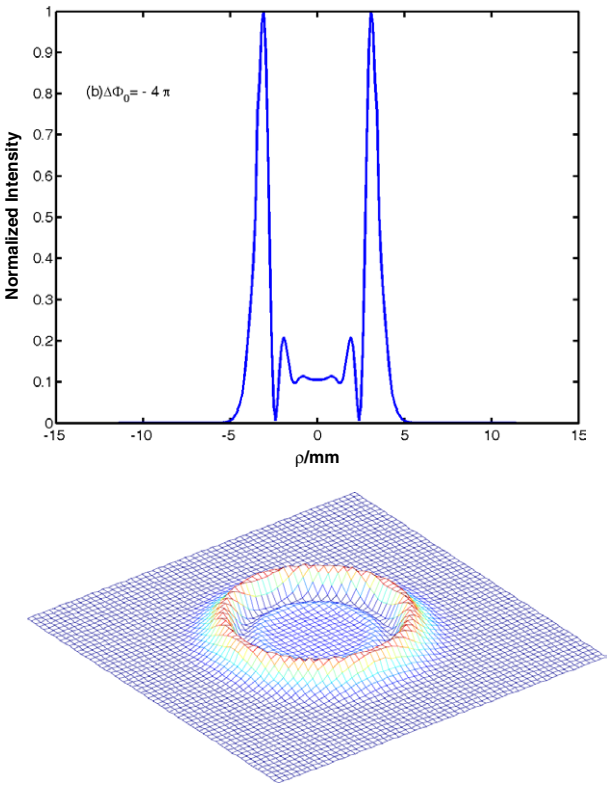

Figure 2. Calculation of the intensity distribution in the far field when the peak-value phase shift $\Delta\phi_0(z_0) = -4\pi$ and the curvature radius $R = 1.33$ m.

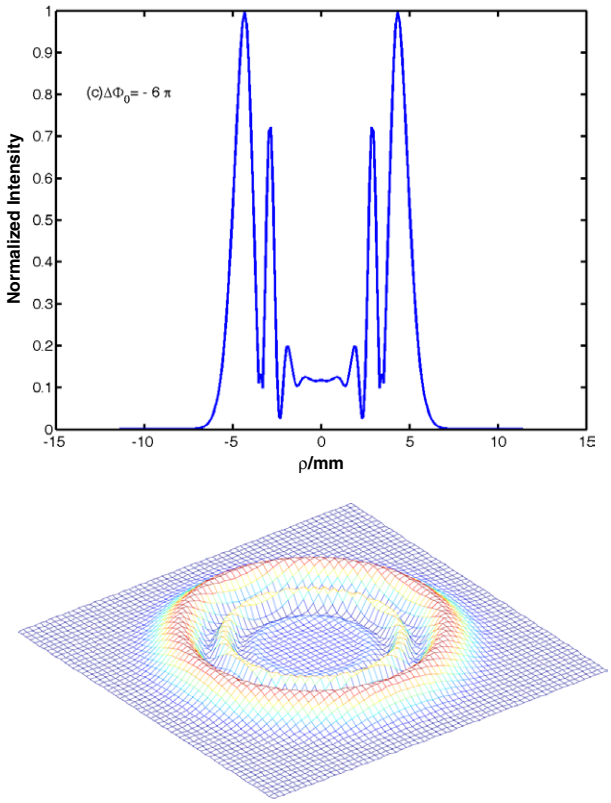

Figure 3. Calculation of the intensity distribution in the far field when the peak-value phase shift $\Delta\phi_0(z_0) = -6\pi$ and the curvature radius $R = 1.33$ m.

beam passes through the medium. If $\Delta n > 0$, the self-phase modulation triggered by Δn will produce a 'positive lens' effect that will cancel out the linear diffraction effect of the Gaussian beam and make the beam focused. If $\Delta n < 0$, the self-phase modulation triggered by Δn will induce a 'negative lens' effect that will aggravate the beam divergence caused by the linear diffraction effect of the Gaussian beam and make the beam diverge. Therefore, the medium with the positive Δn is referred to as the self-focusing medium, while the medium with the negative Δn is called the self-defocusing medium.

It can be seen from equation (2) that, when the Gaussian beam is transmitted through the self-defocusing media, $\Delta\phi(r) < 0$; while, when the Gaussian beam is through the self-focusing media, $\Delta\phi(r) > 0$. Additionally, the Gaussian beam is convergent before the focal plane of the focusing lens and the radius of wavefront curvature $R < 0$; while the beam is divergent behind the focal plane and the radius of curvature $R > 0$. Using equation (8), we can simulate and discuss the various situations for the divergent ($R > 0$) and convergent ($R < 0$) Gaussian beams passing through the self-defocusing and the self-focusing media, respectively. Apparently, there are only four possible sign combinations at most for $\Delta\phi(r)$ and R, that is, (a) $\Delta\phi(r) < 0$, $R > 0$; (b) $\Delta\phi(r) > 0$, $R > 0$; (c) $\Delta\phi(r) > 0$, $R < 0$; (d) $\Delta\phi(r) < 0$, $R < 0$. Since the sign of the total phase shift $\phi(r)$ do not affect the final integral result in equation (8), the combination (a) is equivalent to the combination (c), and the combination (b) is equivalent to the combination (d). Therefore, for simplicity, we will only study the first two situations among the four possible combinations in the following. Theoretically, the distance D between the exit plane of the medium and the far-field observational plane can be chosen arbitrarily. Without any loss of generality, we choose $D = 2.28$ m. In addition, we set $n_0 = 1$, $R = 1.33$ m, $w_p = 1$ mm, $\lambda = 514.5$ nm in the following entire computations.

3.1. $\Delta\phi(r) < 0$, $R > 0$

Figures 1–4 are the typical simulation results for the far-field intensity distribution corresponding to the different peak additional phase shifts $\Delta\phi_0(z_0)$ when the divergent Gaussian beam acts on the self-defocusing media. In these figures, the transverse coordinate ρ is the radial coordinate on the far-field plane, while the longitudinal coordinate denotes the normalized intensity.

The peak additional phase shift $\Delta\phi_0(z_0)$ is equal to -2π in figure 1. It can be spotted from figure 1 that a dark spot emerges around the central area of the transverse coordinate. The intensity of the dark spot is approximately 20% of the peak intensity of the optical field. There exists a bright ring outside the dark spot. In figure 2, the peak additional phase shift $\Delta\phi_0(z_0)$ is decreased to -4π. It can be seen that the central zone of the transverse coordinate is again a dark spot whose range is almost the same as that of figure 1. The intensity is dropped to 10% of the peak intensity. There are two bright rings that occur outside the dark spot. In figure 3, the value of $\Delta\phi_0(z_0)$ is -6π. The range and the normalized intensity of the dark spot are roughly unchanged compared with those of the

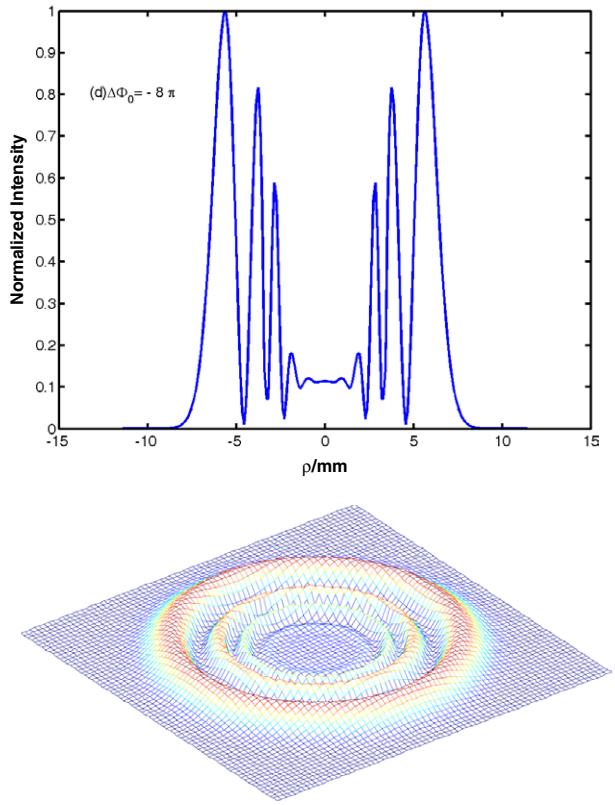

Figure 4. Calculation of the intensity distribution in the far field when the peak-value phase shift $\Delta\phi_0(z_0) = -8\pi$ and the curvature radius $R = 1.33$ m.

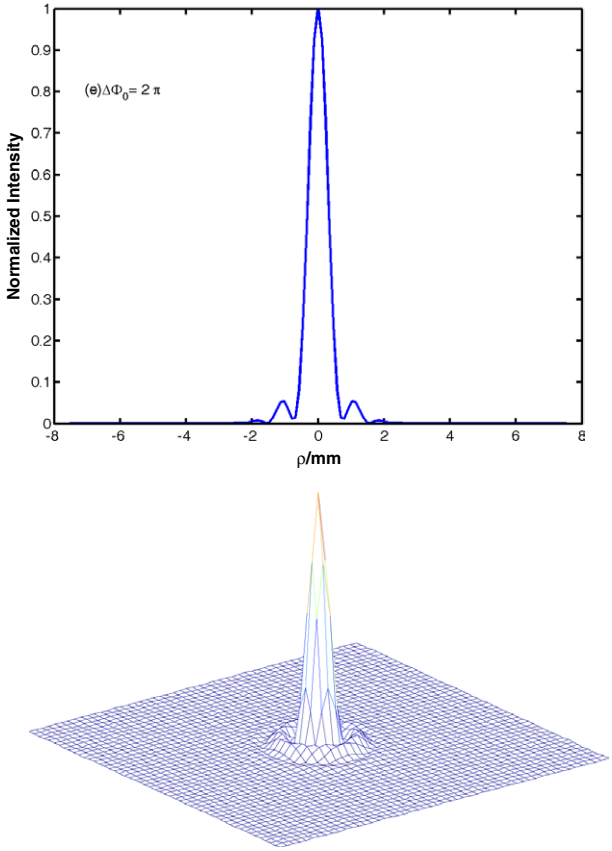

Figure 5. Calculation of the intensity distribution in the far field when the peak-value phase shift $\Delta\phi_0(z_0) = 2\pi$ and the curvature radius $R = 1.33$ m.

dark spot in figure 2, but the number of bright rings surrounding the dark spot is increased to 3 from 2 in figure 2. In addition, the bright diffraction ring becomes thicker gradually from the inner to the outer side and the light energy distributes mainly in the outermost ring. The diffraction pattern ranges from -7 to 7 mm, which is slightly larger than the distribution ranges of the patterns in figures 2 and 1. In figure 4, the value of $\Delta\phi_0(z_0)$ becomes -8π. It can be found that, apart from some common features similar to those of the preceding three figures, one more bright ring occurs in this figure and the total number of bright rings has risen to 4. Not only does the bright diffraction ring become thicker gradually from the inner to the outer side, but the interval between the rings also becomes larger. Because of the increase in the bright ring number, the distribution range of the diffraction pattern increases apparently compared with that of the pattern in the figure 3 and the optical energy is concentrated within a range from -9 to 9 mm including the central dark spot.

It can be seen from the four figures discussed above that the central zones of all the figures are the dark spot and the size of the dark spot is hardly affected by the change in the absolute value of the peak additional phase shift $\Delta\phi_0(z_0)$. With increasing phase shift $\Delta\phi_0(z_0)$, the number of bright diffraction rings around the dark spot increases correspondingly. The relation of the ring number N and the phase shift $\Delta\phi_0(z_0)$ satisfies $N = |\Delta\phi_0(z_0)|/2\pi$. Moreover, not only does the diffraction ring become both thicker and brighter, but the interval between the rings also increases gradually from the pattern centre to the outermost area. It can also be found that as long as the absolute value of the phase shift $\Delta\phi_0(z_0)$ is large enough, the intensity of the dark spot will be retained at about 10% of the normalized peak intensity. In addition, most of the light energy is diffracted into the outermost ring.

3.2. $\Delta\phi(r) > 0, R > 0$

Figures 5–8 are the simulation results for the far-field intensity distribution corresponding to the different peak additional phase shifts $\Delta\phi_0(z_0)$ when the divergent Gaussian beam interplays with the self-focusing media. In figure 5, the peak additional phase shift $\Delta\phi_0(z_0)$ is equal to 2π, while in figures 6–8, the peak phase shift $\Delta\phi_0(z_0)$ is equal to 4π, 6π and 8π, respectively. The radius of the wavefront curvature R in all four figures is 1.33 m. The transverse coordinate ρ denotes the radial coordinate on the far-field plane and the longitudinal coordinate stands for the far-field normalized intensity. Apparently, the current results are completely different from those shown in figures 1–4. It can be seen from figures 5–8 that the intensity maximum of the far field locates at the centre of the diffraction pattern. The greater the distance to the centre, the smaller the peak intensity of the diffraction rings. With increasing phase shift $\Delta\phi_0(z_0)$, the number of diffraction rings does not obey the relation referred to in the above section. That is, the ring number $N \neq |\Delta\phi_0(z_0)|/2\pi$. A similarity with

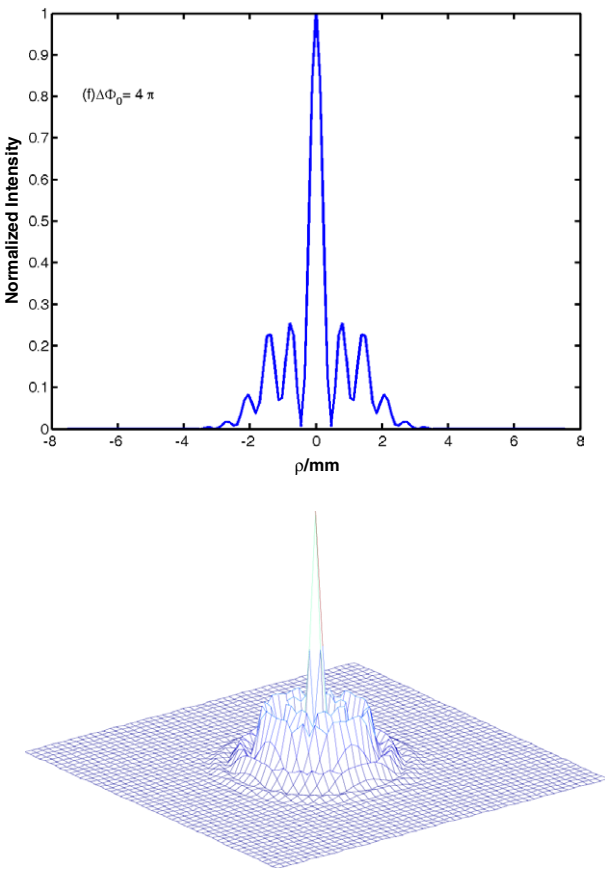

Figure 6. Calculation of the intensity distribution in the far field when the peak-value phase shift $\Delta\phi_0(z_0) = 4\pi$ and the curvature radius $R = 1.33$ m.

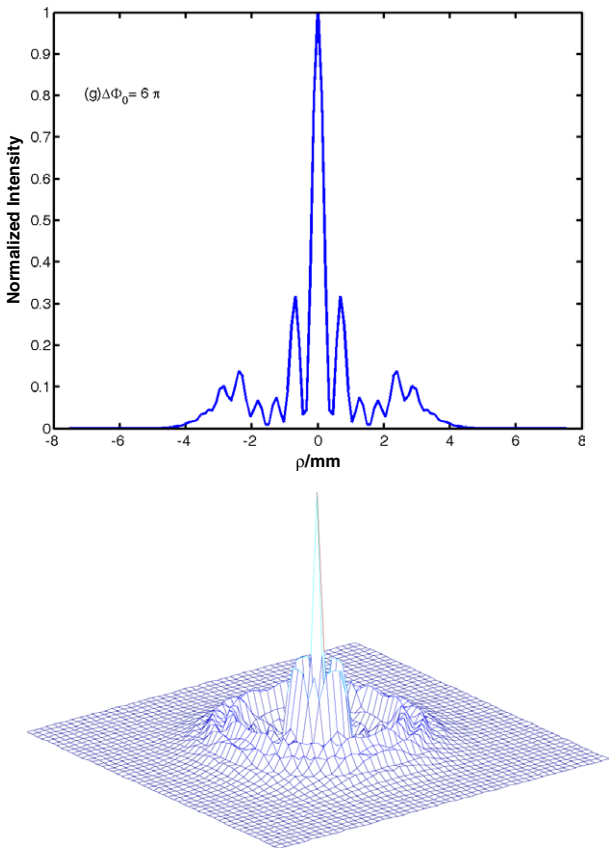

Figure 7. Calculation of the intensity distribution in the far field when the peak-value phase shift $\Delta\phi_0(z_0) = 6\pi$ and the curvature radius $R = 1.33$ m.

the results presented in section 3.1 is that the diffraction ring number increases with increasing absolute value of the phase shift $\Delta\phi_0(z_0)$ and the interval between the rings becomes larger obviously from the inner to the outer region.

It can be seen from figure 5 that there is only a quite weak bright ring outside the central bright spot. The entire pattern is within the range of about ± 1.5 mm. In figures 6–8, with increasing phase shift $\Delta\phi_0(z_0)$, a set of obvious thin diffraction rings whose intensity is much smaller than that of the central bright spot emerge round the outside of the central bright spot. In the range of about ± 1 mm, the diffraction patterns corresponding to figures 6–8 stay almost unchanged. Outside the range of ± 1 mm, the intensity of the diffraction rings decreases rapidly with increasing phase shift $\Delta\phi_0(z_0)$ and the interval between the rings becomes notably thicker. The ring intervals within the range of ± 1 mm are obviously less than those outside the range. Moreover, compared with the distribution range of the diffraction patterns shown in figures 1–4, the intensity distribution zones of the current four diffraction patterns are appreciably smaller and the bright rings are also thinner. In fact, the simulation results shown in figures 5–8 are just the so-called thin diffraction rings, while those shown in figures 1–4 are the so-called thick diffraction rings.

Since the simulation results for the combination ($\Delta\phi(r) > 0$, $R < 0$) and the combination ($\Delta\phi(r) < 0$, $R < 0$) are the same as those shown in sections 3.1 and 3.2, respectively, we do not repeat them here.

4. Conclusion

We have studied the far-field diffraction pattern formation and evolution of the Gaussian beam passing through nonlinear media by the numerical method. We have found that whether the central dark spot and the central bright spot form or not will mainly depend on the sign of the product of the additional phase shift $\Delta\phi(r)$ and the radius of the wavefront curvature R as long as the radius of curvature R is not too large. When the sign of the phase shift $\Delta\phi(r)$ is opposite to that of the curvature radius R, that is, when the divergent Gaussian beam passes through the self-defocusing media, or the convergent Gaussian beam passes through the self-focusing media, the thick diffraction ring pattern with both the central dark spot and the larger distribution range will emerge in the far-field plane; while, when the sign of the phase shift $\Delta\phi(r)$ is identical to that of the curvature radius R, that is, when the divergent Gaussian beam transmits through the self-focusing media, or the convergent Gaussian beam passes through the self-defocusing media, the thin diffraction ring pattern with both the central bright spot and the smaller distribution range will emerge in the far-field plane. The thick diffraction rings mentioned by some authors refer to the large diffraction ring pattern with the central dark spot, and the thin diffraction rings refer to the small diffraction ring pattern with the central bright spot. Both of them can be characterized and calculated using equations (5) and (8).

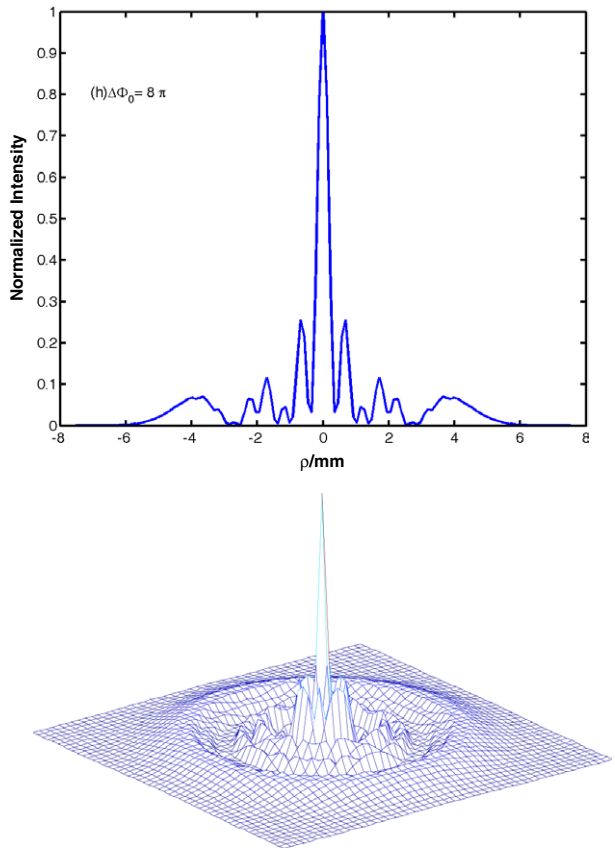

Figure 8. Calculation of the intensity distribution in the far field when the peak-value phase shift $\Delta\phi_0(z_0) = 8\pi$ and the curvature radius $R = 1.33$ m.

The value of the peak additional phase shift $\Delta\phi_0(z_0)$ affects the number of the diffraction rings. By reading off the number of the rings we can estimate the magnitude of the nonlinear coefficient of the materials. Because the changes in the refractive index $\Delta n(z, r)$ and the phase shift $\Delta\phi(r)$ triggered by different mechanisms depend on different material parameters [5, 12], we can study the relation between the relevant parameters responsible for the refractive index change and the optical field intensity distribution by means of the phase shift expression for different mechanisms and equation (8).

In addition, whether the central area of the far-field diffraction pattern is the dark spot or the bright spot, the energy entering the detector placed in the far field is merely a fraction of the total incident energy. However, from the viewpoint of the optical limitation, we prefer large diffraction rings with the central dark spot, so as to protect the detector effectively. Therefore, the condition that the sign of the product of the phase shift $\Delta\phi(r)$ and the curvature radius R is less than 0 must be satisfied for a good optical limiter. Therefore, if the optical limiting material used is a self-defocusing medium, we must install the sample cell behind the focus and before the detector; otherwise, if the material is a self-focusing medium, we must place it between the focusing lens and the focus.

Acknowledgments

This work was supported by the National Natural Science Foundation of China under Grant No. 10474006. We appreciate the helpful technical discussions with Professor Chunfei Li and Hua-Kuang Liu.

References

[1] Callen W R, Huth B G and Pantell R H 1967 Optical patterns of thermally self-defocused light *Appl. Phys. Lett.* **11** 103–5
[2] Durbin S D, Arakelian S M and Shen Y R 1981 Laser-induced diffraction rings from a nematic-liquid-crystal film *Opt. Lett.* **6** 411–3
[3] Dabby F W, Gustafson T K, Whinnery J R and Kohanzadeh Y 1970 Thermally self-induced phase modulation of laser beams *Appl. Phys. Lett.* **16** 362–5
[4] Santamato E and Shen Y R 1984 Field-curvature effect on the diffraction ring pattern of a laser beam dressed by spatial self-phase modulation in a nematic film *Opt. Lett.* **9** 564–6
[5] Yao B L, Ren L Y, Hou X, Yi W H and Wang M Q 2001 Diffraction behavior of poly-pyrrylarylenmethine/polyvinyl film to Gaussian beam *Acta Opt. Sin.* **21** 1139–43
[6] Ono H and Kawatsuki N 1997 Controllable optical intensity limiting of a He–Ne laser with host–guest liquid crystals *Opt. Commun.* **139** 60–2
[7] Deng L G and Liu H K 2003 Nonlinear optical limiting of the azo dye methyl red doped nematic liquid crystalline films *Opt. Eng.* **42** 2936–41
[8] Song Y, Milam D and Hill W T III 1999 Long, narrow all-light atom guide *Opt. Lett.* **24** 1805–7
[9] Ozeri R, Khaykovich L, Friedman N and Davidson N 2000 Large-volume single-beam dark optical trap for atoms using binary phase elements *J. Opt. Soc. Am.* B **17** 1113–6
[10] Shevchenko A, Buchter S C, Tabiryan N V and Kaivola M 2004 Creation of a hollow laser beam using self-phase modulation in a nematic liquid crystal *Opt. Commun.* **232** 77–82
[11] Watanabe T, Lgasaki Y, Sakai M, Ishiuchi S I, Fujii M, Omatsu T, Yamamoto K and Iketaki Y 2004 Formation of a doughnut laser beam for super-resolving microscopy using a phase spatial light modulator *Opt. Eng.* **43** 1136–43
[12] Yu D J, Lu W P and Harrison R G 1998 Analysis of dark spot formation in absorbing liquid media *J. Mod. Opt.* **45** 2597–606
[13] Khoo I C, Finn G M, Michael R R and Liu T H 1986 Passive optical self-limiter using laser-induced axially asymmetric and symmetric transverse self-phase modulations in nematic liquid crystals *Opt. Lett.* **11** 227–9
[14] Khoo I C, Michael R G and Finn G M 1988 Self-phase modulation and optical limiting of a low-power CO_2 laser with a nematic liquid crystal film *Appl. Phys. Lett.* **52** 2108–10
[15] Born M and Wolf E 1980 *Principles of Optics* (Oxford: Pergamon)
[16] Qian S X and Wang G M 2001 *Nonlinear Optics: Principles and Progress* (Shanghai: Fudan University Press)
[17] Brugioni S and Meucci R 2002 Self-phase modulation in a nematic liquid crystal film induced by a low-power CO_2 laser *Opt. Commun.* **206** 445–51
[18] Ono H and Harato Y 1999 Anisotropic diffraction pattern formation from guest–host liquid crystals *Opt. Commun.* **168** 251–9
[19] Castaldo F, Paparo D and Santamato E 1997 Chaotic and hexagonal spontaneous pattern formation in the cross section of a laser beam in a defocusing Kerr-like film with single feedback mirror *Opt. Commun.* **143** 57–61